Multiparameter Estimation Perspective on Non-Hermitian Singularity-Enhanced Sensing

Javid Naikoo,[1,*] Ravindra W. Chhajlany,[2,1] and Jan Kołodyński[1,†]

[1]*Centre for Quantum Optical Technologies, Centre of New Technologies, University of Warsaw, Banacha 2c, 02-097 Warszawa, Poland*

[2]*Institute of Spintronics and Quantum Information, Faculty of Physics, Adam Mickiewicz University, 61-614 Poznań, Poland*

(Received 3 April 2023; accepted 6 November 2023; published 29 November 2023)

Describing the evolution of quantum systems by means of non-Hermitian generators opens a new avenue to explore the dynamical properties naturally emerging in such a picture, e.g. operation at the so-called exceptional points, preservation of parity-time symmetry, or capitalizing on the singular behavior of the dynamics. In this Letter, we focus on the possibility of achieving unbounded sensitivity when using the system to sense linear perturbations away from a singular point. By combining multiparameter estimation theory of Gaussian quantum systems with the one of singular-matrix perturbations, we introduce the necessary tools to study the ultimate limits on the precision attained by such singularity-tuned sensors. We identify under what conditions and at what rate can the resulting sensitivity indeed diverge, in order to show that nuisance parameters should be generally included in the analysis, as their presence may alter the scaling of the error with the estimated parameter.

DOI: 10.1103/PhysRevLett.131.220801

Introduction.—Quantum entanglement boosts dramatically performance in sensing [1,2], allowing quantum sensors to breach classical limits imposed by the independent identically distributed statistics [3]. The corresponding enhancement, however, turns out to be very fragile [4–6], making methods of quantum control [7–9] and error correction [10–12] essential, if the robustness against decoherence and imperfections is to be maintained. As the impact of noise becomes inevitable with sensor complexity, a change of paradigm is necessary. One way is to adopt a non-Hermitian dynamical description and engineer the noise instead, in order to make the evolution extremely sensitive to external perturbations. For example, considering deviations from *exceptional points* (EPs) in the space of parameters characterizing the system [13]—special degeneracies at which n (complex) eigenvalues coalesce along with their eigenmodes [14–16]—a linear perturbation ϵ away from the EP leads to an nth-root splitting $\sim\sqrt[n]{\epsilon}$ of the eigenmode frequencies [17]. Hence, a splitting measurement may yield infinitely steep signals of unbounded sensitivity as $\epsilon \to 0$, as demonstrated with optical resonators [18,19] in the regime in which the measurement-induced noise can be ignored. Otherwise, the effect is washed out by the quantum noise [20–22]—in a similar way as it prohibits noiseless amplification of optical signals [23,24].

Alternative schemes involving linearly coupled systems were proposed (cf. [25]) that surpass the impact of quantum noise by resorting to perturbations of the effective non-Hermitian generator, $\mathbf{H}$, in the Langevin formalism [26]—with the operation around an EP being no longer essential [27]. For example, by considering the internal interaction to be nonreciprocal and perturbing the coupling strength, the sensitivity—the signal-to-noise ratio (SNR)—was shown to improve by a constant factor [29]. Moreover, it was shown that by engineering $\mathbf{H}$ to be *singular* [30] and sensing perturbations of the internal frequency probed on resonance, the SNR may diverge boundlessly as ϵ^{-2} with $\epsilon \to 0$ [31]. Despite the similarity to the EP-induced effect, this is a consequence of probing the sensor close to a dynamical phase transition useful for sensing [32–39]. Although linearity of dynamics may be questioned at a critical point [17,20], it is valid at different probe powers [40] for sensors we consider [40–44].

Here, we demonstrate how to correctly assess singularity-tuned sensors [31], opening doors for other criticality-enhanced schemes [32–39]. We investigate singularity-induced SNR-divergence in a linear system exhibiting parity-time (PT) symmetry [45]: two coupled bosonic cavities experiencing loss and gain [40–44]; see Fig. 1. Its non-Hermitian dynamics allows EP- [17], nonreciprocity- [29], and singularity-based [31] sensing. We employ multiparameter estimation theory of multimode Gaussian states [46] to determine sensitivity limits. By performing singular perturbations [47–50] of the corresponding response function, we show that the critical behavior of the SNR at the singularity depends not only on the perturbation form but also on nuisance parameters unknown prior to estimation [51,52].

Non-Hermitian sensor model.—Sensors [40–44] can be described by the model depicted in Fig. 1, in which two cavities containing modes $\hat{a}_1$ and $\hat{a}_2$ at frequencies ω_1 and ω_2, respectively, are linearly coupled with strength g, so that the Hamiltonian reads

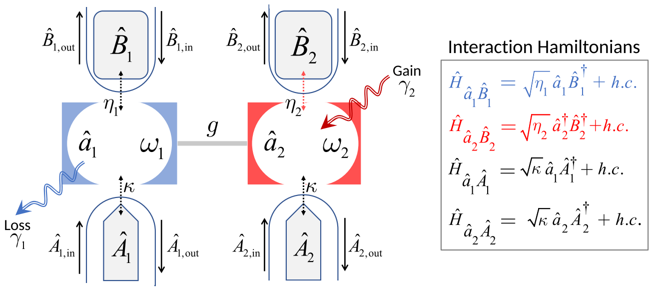

FIG. 1. Non-Hermitian sensor model consisting of two coupled cavities bearing modes $\hat{a}_1$ and $\hat{a}_2$ with effective loss and gain rates $\gamma_1 = [(\eta_1 + \kappa)/2]$ and $\gamma_2 = [(\eta_2 - \kappa)/2]$. The rates are controlled by "scattering channels" (modes), $\hat{B}_1$ and $\hat{B}_2$, coupled to respective cavities, whose dynamics is also affected by "probing channels", $\hat{A}_1$ and $\hat{A}_2$, used to continuously monitor each cavity.

$$\hat{H}_S = \omega_1 \hat{a}_1^\dagger \hat{a}_1 + \omega_2 \hat{a}_2^\dagger \hat{a}_2 + g\left(\hat{a}_1^\dagger \hat{a}_2 + \hat{a}_2^\dagger \hat{a}_1\right). \qquad (1)$$

We consider here degenerate cavities with $\omega_1 = \omega_2 =: \omega_0$ [40]. Each mode $\hat{a}_1$ ($\hat{a}_2$) is separately coupled to a scattering channel $\hat{B}_1$ ($\hat{B}_2$) that effectively induces loss (gain) of strength η_1 (η_2) on each cavity. The couplings correspond to effective beam-splitter and nondegenerate parametric-amplifier [53] interactions, see Fig. 1, with other nonlinear effects being ignored [54]. In parallel, both cavities are independently probed via channels $\hat{A}_1$ and $\hat{A}_2$, each coupled with strength κ, whose outputs are monitored. By resorting to input-output formalism [55,56], the sensor dynamics is described by a linear quantum Langevin equation [26,57]:

$$\partial_t \hat{\boldsymbol{a}} = -\mathrm{i}(\omega_0 \mathbf{I} + \mathbf{H})\hat{\boldsymbol{a}} + \hat{\boldsymbol{A}}_{\mathrm{in}} + \hat{\boldsymbol{B}}_{\mathrm{in}}, \qquad (2)$$

where $\hat{\boldsymbol{a}} := \{\hat{a}_1, \hat{a}_2\}^{\mathrm{T}}$, $\hat{\boldsymbol{A}}_{\mathrm{in}} := \{\sqrt{\kappa}\hat{A}_{1,\mathrm{in}}, \sqrt{\kappa}\hat{A}_{2,\mathrm{in}}\}^{\mathrm{T}}$, $\hat{\boldsymbol{B}}_{\mathrm{in}} := \{\sqrt{\eta_1}\hat{B}_{1,\mathrm{in}}, -\sqrt{\eta_2}\hat{B}_{2,\mathrm{in}}^\dagger\}^{\mathrm{T}}$, and $\mathbf{I}$ is a 2×2 identity matrix. $\hat{A}_{\ell,\mathrm{in}}$, $\hat{B}_{\ell,\mathrm{in}}$ with $\ell = 1, 2$ denote the effective input fields of the optical channels, see Fig. 1, whose output fields are determined by input-output relations [26] and read at time t: $\hat{A}_{\ell,\mathrm{out}}(t) = \hat{A}_{\ell,\mathrm{in}}(t) - \sqrt{\kappa}\hat{a}_\ell(t)$ [57].

The evolution of the cavity modes in Eq. (2) is described by the non-Hermitian dynamical generator that reads

$$\mathbf{H} = \begin{pmatrix} -\mathrm{i}\gamma_1 & g \\ g & +\mathrm{i}\gamma_2 \end{pmatrix}, \qquad (3)$$

with $\gamma_1 := (\eta_1 + \kappa)/2(\gamma_2 := (\eta_2 - \kappa)/2)$ being the overall loss (gain) rate of each cavity. As a result, defining $\gamma_\pm := (\gamma_2 \pm \gamma_1)/2$, the eigenvalues and eigenmodes of $\mathbf{H}$ read

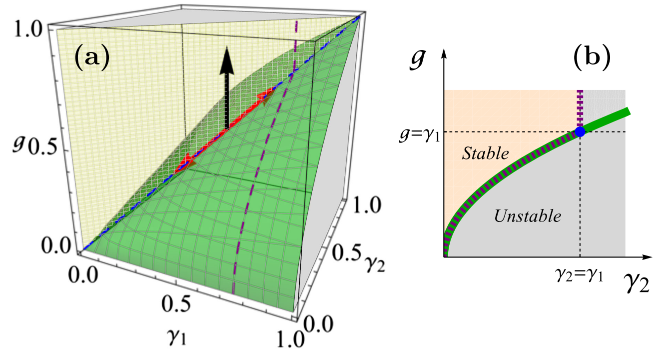

FIG. 2. Space of parameters characterizing the dynamical generator $\mathbf{H}$ in Eq. (3), with g and γ_1 (γ_2) being the coupling constant and loss (gain) rates, respectively. (a) The green surface depicts values where the singularity condition $\det \mathbf{H} = 0$ holds, and the triangular plane represents PT symmetry. Their intersection, where $g = \gamma_1 = \gamma_2$, guarantees the EP condition (dashed blue line). (b) Cut at $\gamma_1 = 0.75$ is included to show the separation between stable and unstable regions of dynamics—with the lasing threshold (purple dashed line) following the singularity surface before becoming (at an EP, blue dot) equivalent to the PT condition for $g > \gamma_1$. In the multiparameter estimation setting, we consider nuisance parameters to preserve PT symmetry while either invalidating (black arrow) or maintaining (red arrows) the singularity condition.

$$\lambda_\pm = \mathrm{i}\gamma_- \pm \sqrt{g^2 - \gamma_+^2}, |e_\pm\rangle = \begin{pmatrix} -\mathrm{i}\gamma_+ \pm \sqrt{g^2 - \gamma_+^2} \\ g \end{pmatrix}, \qquad (4)$$

so that the spectrum of $\mathbf{H}$ is real if and only if $g \geq \gamma_+$ and $\gamma_- = 0$, in which case $\mathbf{H}$ formally exhibits PT symmetry [45]. The PT condition is conveniently visualized in $\{\gamma_1, \gamma_2, g\}$ parameter space, see Fig. 2(a), by a vertical (yellow) triangular plane. Importantly, by maintaining the PT symmetry the validity of the linear model (2) can be extended to high probe powers [40]. The sole condition $\gamma_- = 0$ we term as the balanced scenario, as the gain then balances out exactly the loss ($\gamma_1 = \gamma_2$) [43]. In what follows, when probing the system at the sensor frequency ω_0, the *singularity* of the non-Hermitian generator (3) will play a pivotal role. This corresponds to the condition $\det \mathbf{H} = 0$ or $g^2 = \gamma_1\gamma_2$, represented by the green surface in Fig. 2(a). Contrarily, $\mathbf{H}$ exhibits an EP at $g = \gamma_+$ when both $\lambda_\pm$ and $|e_\pm\rangle$ coalesce [45]. In Fig. 2(a), we mark the EP condition when singularity is also fulfilled (dashed blue line). The constant-γ_1 cut in Fig. 2(b) shows singularity and PT-symmetry conditions separate $\mathrm{Im}\lambda_\pm$ into negative or positive regions, determining stable or unstable dynamics, respectively. The $\mathrm{Im}\lambda_\pm = 0$ border defines the lasing threshold [43] (marked for $\gamma_1 = 0.75$ by dashed purple line), which for $g > \gamma_1$ does not occur at the singularity [57].

In sensing tasks with linear perturbations, the generator (3) is modified as follows:

$$\mathbf{H}_{\boldsymbol{\theta}} := \mathbf{H} - \sum_i \theta_i \mathbf{n}_i = \mathbf{H}_{\bar{\boldsymbol{\theta}}} - \theta_0 \mathbf{n}_0, \tag{5}$$

where $\boldsymbol{\theta} := \{\theta_i\}_i$ denotes a set of (real) parameters to be sensed, each of which modifies $\mathbf{H}$ according to some (complex) 2×2 matrix $\mathbf{n}_i$. In Eq. (5), we single out the case in which θ_0 denotes the primary parameter to be sensed around zero, while the rest of the set, $\bar{\boldsymbol{\theta}} := \{\theta_i\}_{i\neq 0}$, contains nuisance parameters, i.e. ones that are of no interest but nonetheless unknown. This allows us to capture the following θ_0-estimation scenarios: by setting $\mathbf{n}_0 = \sigma_z$ in Eq. (5), we let $\theta_0 = (\omega_1 - \omega_2)/2$ describe perturbations of the detuning between the cavity frequencies—as originally considered in the EP-based sensing schemes [20]; by choosing $\mathbf{n}_0 = \sigma_x$, we let θ_0 perturb the coupling strength g—as investigated in Ref. [29] dealing with nonreciprocal dynamics; when $\mathbf{n}_0 = \mathbf{I}$ $[\mathbf{n}_0 = (1,0;0,0)]$ θ_0 describes perturbations of the common frequency ω_0 (of ω_1 for the first cavity only) [31].

Linear response in the Fourier domain.—We consider the sensor to be interacting with Gaussian light [58], so it is sufficient to describe its dynamics using the Gaussian formalism [59,60], within which evolution of bosonic modes $\hat{b}_i$ is fully characterized after defining the vector $\hat{\mathsf{S}} = \{\hat{q}_1, \hat{q}_2, \ldots, \hat{p}_1, \hat{p}_2, \ldots\}^{\mathrm{T}}$ of their quadratures, $\hat{q}_i = \hat{b}_i + \hat{b}_i^\dagger$ and $\hat{p}_i = -\mathrm{i}(\hat{b}_i - \hat{b}_i^\dagger)$, and tracking its mean $\mathsf{S} := \langle \hat{\mathsf{S}} \rangle$ and covariance V with entries $\mathsf{V}_{jk} := \frac{1}{2}\langle\{\hat{\mathsf{S}}_j, \hat{\mathsf{S}}_k\}\rangle - \langle\hat{\mathsf{S}}_j\rangle\langle\hat{\mathsf{S}}_k\rangle$. As we are interested in probing the sensor at a particular frequency ω, we focus on the evolution in the Fourier space, in which according to Eq. (2) the dynamics of measured outputs, $\hat{\mathsf{S}}^A_{\mathrm{out}}$ containing quadratures of $\hat{A}_{\ell,\mathrm{out}}[\omega] := \int \mathrm{d}t\, \mathrm{e}^{\mathrm{i}\omega t} \hat{A}_{\ell,\mathrm{out}}(t)$, is given by $\mathsf{S}^A_{\mathrm{out}} = (\mathsf{I} - \kappa \mathsf{G})\mathsf{S}^A_{\mathrm{in}}$ and $\mathsf{V}^A_{\mathrm{out}} = (\mathsf{I} - \kappa\mathsf{G})\mathsf{V}^A_{\mathrm{in}}(\mathsf{I} - \kappa\mathsf{G})^{\mathrm{T}} + \kappa \mathsf{G}\Xi\tilde{\mathsf{V}}^B_{\mathrm{in}}\Xi^{\mathrm{T}}\mathsf{G}^{\mathrm{T}}$. The covariance of probe outputs $\mathsf{V}^A_{\mathrm{out}}$ depends also on the covariance of input scattering modes, i.e. $\tilde{\mathsf{V}}^B_{\mathrm{in}}$ describing correlations between eight quadratures ($\ell = 1,\ 2$) of $\hat{B}_{\ell,\mathrm{in}}[\pm\omega]$ [57]. The matrix Ξ is associated with the coupling of cavities to scattering channels, I denotes a 4×4 identity matrix, while the central object is the (linear-) response function,

$$\mathsf{G}[\omega] = \mathsf{J}[(\omega - \omega_0)\mathsf{I} - \mathsf{H}]^{-1}, \tag{6}$$

whose divergent behavior will be responsible for the unbounded precision when sensing perturbations. By $\mathsf{J} = (0, -\mathbf{I}; \mathbf{I}, 0)$ we denote the symplectic form consistently with the notation of [57], within which [61]

$$\mathsf{H} := \begin{pmatrix} \mathrm{Re}[\mathbf{H}] & -\mathrm{Im}[\mathbf{H}] \\ \mathrm{Im}[\mathbf{H}] & \mathrm{Re}[\mathbf{H}] \end{pmatrix} = \begin{pmatrix} 0 & g & \gamma_1 & 0 \\ g & 0 & 0 & -\gamma_2 \\ -\gamma_1 & 0 & 0 & g \\ 0 & \gamma_2 & g & 0 \end{pmatrix} \tag{7}$$

is the phase-space representation of $\mathbf{H}$. Equation (6) diverges if $\det[(\omega - \omega_0)\mathsf{I} - \mathsf{H}] = 0$, which can always be assured by tuning loss and gain, as long as the probing is performed *in resonance* ($\omega = \omega_0$) with the common internal frequency. Divergence then occurs when $\det \mathsf{H} = |\det \mathbf{H}|^2 = 0$, i.e. when the generator $\mathbf{H}$ in (3) is, indeed, singular [62].

Considering now $\boldsymbol{\theta}$-parametrized perturbations specified in Eq. (5), the response function (6) becomes

$$\mathsf{G}_{\boldsymbol{\theta}}[\omega = \omega_0] = \mathsf{J}\left(\sum\nolimits_i \theta_i \mathsf{n}_i - \mathsf{H}\right)^{-1} = \mathsf{J}(\theta_0 \mathsf{n}_0 - \mathsf{H}_{\bar{\boldsymbol{\theta}}})^{-1}, \tag{8}$$

where n_i are the phase-space representations of $\mathbf{n}_i$ [61]. Analogously to Eq. (5), we highlight the case when θ_0 is the primary parameter and $\mathsf{H}_{\bar{\boldsymbol{\theta}}} := \mathsf{H} - \sum_{i\neq 0}\theta_i \mathsf{n}_i$. For singular dynamics with $\det \mathsf{H} = 0$, the response function (8) diverges when all $\theta_i = 0$, but the form of divergence depends on $\{\mathsf{n}_i\}_i$. For example, when estimating $\theta_0 \approx 0$ the singularity may be maintained despite $\bar{\boldsymbol{\theta}} \neq 0$, as long as $\det \mathsf{H}_{\bar{\boldsymbol{\theta}}} = 0$ also for $\bar{\boldsymbol{\theta}} \neq 0$.

Aiming to study such subtleties and treat $\bar{\boldsymbol{\theta}}$ as nuisance parameters, we focus on the *two-parameter* setting, $\boldsymbol{\theta} = \{\theta_0, \theta_1\}$, in which the primary parameter represents ω_0-frequency perturbations, i.e. $\mathbf{n}_0 = \mathbf{I}$ [31]. In contrast, we choose the secondary parameter θ_1 such that its variations either invalidate or maintain the singularity condition but do not break the PT symmetry, so that the linearity of dynamics is ensured [40]. In Fig. 2(a), we mark these cases by black and red arrows, respectively, which correspond to singularity nonpreserving (NS) increase of the coupling g [29], and singularity preserving (S) perturbations maintaining $g = \gamma_1 = \gamma_2$ and, hence, the EP condition [63]. The two scenarios yield Eq. (5) of the form $\mathbf{H}_{\boldsymbol{\theta}} = \mathbf{H}^{\mathrm{NS/S}}_{\theta_1} - \theta_0 \mathbf{I}$, where

$$\mathbf{H}^{\mathrm{NS}}_{\theta_1} := \bar{\mathbf{H}} - \theta_1 \sigma_x \quad \text{and} \quad \mathbf{H}^{\mathrm{S}}_{\theta_1} := \bar{\mathbf{H}} - \theta_1(\sigma_x - \mathrm{i}\sigma_z), \tag{9}$$

and $\bar{\mathbf{H}}$ denotes $\mathbf{H}$ with $g = \gamma_1 = \gamma_2 = 1$ [64].

Multiparameter estimation of Gaussian states.—For a quantum system prepared in a state $\rho_{\boldsymbol{\theta}}$ parametrized by $\boldsymbol{\theta} := \{\theta_i\}_i$ and a measurement with outcome ξ distributed according to $p(\xi|\boldsymbol{\theta})$, the classical and quantum Fisher information matrices (CFIM and QFIM) read, respectively [51],

$$\boldsymbol{F}_{jk} := \mathbb{E}_{p(\xi|\boldsymbol{\theta})}[\partial_j \ln p(\xi|\boldsymbol{\theta}) \partial_k \ln p(\xi|\boldsymbol{\theta})], \tag{10}$$

$$\boldsymbol{\mathcal{F}}_{jk} := \mathrm{Tr}\left[\rho_{\boldsymbol{\theta}} \frac{1}{2}\{L_j, L_k\}\right], \tag{11}$$

where $\partial_j \equiv \partial/\partial_{\theta_j}$ is the derivative with respect to any estimated parameter θ_j, while by $\mathbb{E}_{p(\xi|\boldsymbol{\theta})}[\bullet] := \int \mathrm{d}\xi\, p(\xi|\boldsymbol{\theta})\bullet$ we denote the expected value. In the quantum case (11),

$\mathbb{E}_{p(\xi|\boldsymbol{\theta})}[\bullet]$ naturally generalizes to $\mathrm{Tr}[\rho_{\boldsymbol{\theta}}\bullet]$, while $\partial_j \ln p(\xi|\boldsymbol{\theta})$ becomes the symmetric logarithmic derivative L_j, defined as the solution to $\partial_j\rho_{\boldsymbol{\theta}} = \frac{1}{2}\{\rho_{\boldsymbol{\theta}}, L_j\}$ [65–67].

For any unbiased estimator $\tilde{\boldsymbol{\theta}}(\boldsymbol{\xi})$ constructed based on measurement data $\boldsymbol{\xi} = \{\xi_r\}_{r=1}^{\nu}$ gathered over ν independent shots, its (squared-)error matrix $\boldsymbol{\Delta}^2\tilde{\boldsymbol{\theta}} \coloneqq \mathbb{E}[(\tilde{\boldsymbol{\theta}} - \boldsymbol{\theta})(\tilde{\boldsymbol{\theta}} - \boldsymbol{\theta})^{\mathrm{T}}]$ satisfies the quantum Cramér-Rao bound [65,66]:

$$\nu\boldsymbol{\Delta}^2\tilde{\boldsymbol{\theta}} \geq \boldsymbol{F}^{-1} \geq \boldsymbol{\mathcal{F}}^{-1}, \tag{12}$$

where the first matrix inequality is guaranteed to be saturable by some $\tilde{\boldsymbol{\theta}}$ in the $\nu \to \infty$ limit, i.e. for any $\boldsymbol{W} \geq 0$ for which $\mathrm{Tr}[\boldsymbol{W}\boldsymbol{\Delta}^2\tilde{\boldsymbol{\theta}}]$ is then minimized. In contrast, although the second inequality applies to any quantum measurement, as the optimal measurements for distinct parameters θ_i may not commute (formally $\mathrm{Tr}[\rho_{\boldsymbol{\theta}}[L_j, L_k]] \neq 0$ [68]), it may *not* be generally saturable by any estimator $\tilde{\boldsymbol{\theta}}$ given some $\boldsymbol{W} \geq 0$. However, it can differ at most by a factor of 2 from the minimal $\mathrm{Tr}[\boldsymbol{W}\boldsymbol{F}^{-1}]$ attained by the optimal measurements [51].

When estimating a single parameter θ_i with others treated as nuisance ones, i.e. $\boldsymbol{W}_{jk} = \delta_{ij}\delta_{ik}$, we denote the lower bounds on the error in Eq. (12) as $\Delta_{\mathrm{C}}\theta_i \coloneqq \sqrt{[\boldsymbol{F}^{-1}]_{ii}}$ and $\Delta_{\mathrm{Q}}\theta_i \coloneqq \sqrt{[\boldsymbol{\mathcal{F}}^{-1}]_{ii}}$, so that any unbiased estimator of θ_i satisfies then $\nu\Delta^2\tilde{\theta}_i \geq \Delta^2_{\mathrm{C}}\theta_i \geq \Delta^2_{\mathrm{Q}}\theta_i$ [69]. This contrasts the *ideal* single-parameter scenario with all parameters known apart from θ_i, in which case Eq. (12) simplifies to $\nu\Delta^2\tilde{\theta}_i \geq \delta^2_{\mathrm{C}}\theta_i \geq \delta^2_{\mathrm{Q}}\theta_i$ with $\delta_{\mathrm{C}}\theta_i \coloneqq 1/\sqrt{[\boldsymbol{F}]_{ii}}$ and $\delta_{\mathrm{Q}}\theta_i \coloneqq 1/\sqrt{[\boldsymbol{\mathcal{F}}]_{ii}}$.

Considering any Gaussian measurement of the probe outputs $\hat{A}_{\ell,\mathrm{out}}$, its outcome x is normally distributed $\mathsf{x} \sim \exp\{-\frac{1}{2}(\mathsf{x} - \bar{\mathsf{x}})\mathsf{C}^{-1}(\mathsf{x} - \bar{\mathsf{x}})^T\}$ [60,71], with both the mean vector $\bar{\mathsf{x}}(\boldsymbol{\theta})$ and the covariance matrix $\mathsf{C}(\boldsymbol{\theta})$ depending on the parameter set $\boldsymbol{\theta}$. The CFIM (10) takes then a special form [72]:

$$\boldsymbol{F}_{jk} = \frac{1}{2}\mathrm{Tr}[\mathsf{C}^{-1}(\partial_j\mathsf{C})\mathsf{C}^{-1}(\partial_k\mathsf{C})] + (\partial_j\bar{\mathsf{x}})^{\mathrm{T}}\mathsf{C}^{-1}(\partial_k\bar{\mathsf{x}}), \tag{13}$$

so that in case of a heterodyne measurement being performed one should replace $\bar{\mathsf{x}} = \mathsf{S}^A_{\mathrm{out}}$ and $\mathsf{C} = \mathsf{V}^A_{\mathrm{out}} + \mathsf{I}$ in the above [60]. More generally, allowing for arbitrary quantum measurements performed on a Gaussian state of mean $\mathsf{S}(\boldsymbol{\theta})$ and covariance $\mathsf{V}(\boldsymbol{\theta})$, the QFIM (11) reads $\boldsymbol{\mathcal{F}}_{jk} = \frac{1}{2}\mathrm{Tr}[\mathsf{L}_j\partial_k\mathsf{V}] + (\partial_j\mathsf{S})^{\mathrm{T}}\mathsf{V}^{-1}(\partial_k\mathsf{S})$ [46,73–76], with the matrix L_j possessing a nontrivial form [57]. However, by generalizing the results of [77] to the multiparameter case, we show that QFIM can always be approximated for noisy Gaussian states, e.g. highly thermalized, as [57,76]

$$\boldsymbol{\mathcal{F}}_{jk} \approx \frac{1}{2}\mathrm{Tr}[\mathsf{V}^{-1}(\partial_j\mathsf{V})\mathsf{V}^{-1}(\partial_k\mathsf{V})] + (\partial_j\mathsf{S})^{\mathrm{T}}\mathsf{V}^{-1}(\partial_k\mathsf{S}), \tag{14}$$

as long as the spectrum of V satisfies $\lambda_{\min}(\mathsf{V}) \gg 1$. In our case, the *noisy QFIM* (14) is then determined by the response function (8), with $\mathsf{S}(\boldsymbol{\theta}) = (\mathsf{I} - \kappa\mathsf{G}_{\boldsymbol{\theta}})\mathsf{S}^A_{\mathrm{in}}$ and $\mathsf{V}(\boldsymbol{\theta}) = (\mathsf{I} - \kappa\mathsf{G}_{\boldsymbol{\theta}})\mathsf{V}^A_{\mathrm{in}}(\mathsf{I} - \kappa\mathsf{G}_{\boldsymbol{\theta}})^{\mathrm{T}} + \kappa\mathsf{G}_{\boldsymbol{\theta}}\Xi\tilde{\mathsf{V}}^B_{\mathrm{in}}\Xi^{\mathrm{T}}\mathsf{G}^{\mathrm{T}}_{\boldsymbol{\theta}}$.

Single-parameter sensitivities.—When sensing a single parameter θ_0 with others perfectly known, we set $\bar{\boldsymbol{\theta}} = 0$ in Eq. (8), so that $\mathsf{H}_{\bar{\boldsymbol{\theta}}=0} = \mathsf{H}$ and only the entry $j = k = 0$ in Eq. (14) is relevant. Now, whenever the generator H is *nonsingular*, the response function (8) admits a Neumann series $\mathsf{G}_{\theta_0} = -\mathsf{J}\mathsf{H}^{-1}[\mathsf{I} + \sum_{k=1}^{\infty}\theta_0^k(\mathsf{n}_0\mathsf{H}^{-1})^k]$ [78] with $\lim_{\theta_0\to 0}\mathsf{G}_{\theta_0} = -\mathsf{J}\mathsf{H}^{-1}$. As a result, Eq. (14) reads $\boldsymbol{\mathcal{F}}_{00} \approx C + \mathcal{O}(\theta_0)$ with some θ_0-independent finite constant C [57], so the error cannot vanish as $\theta_0 \to 0$, at which its minimal value is given by $\delta_{\mathrm{Q}}\theta_0 = 1/\sqrt{C} > 0$ [79]. In contrast, when the generator H is *singular*, the Sain-Massey (SM) expansion [47–50] of the response function (8) applies, i.e. $\mathsf{G}_{\theta_0} = \mathsf{J}\theta_0^{-s}\sum_{k=0}^{r}\theta_0^k\mathsf{X}_k$ with each nonzero coefficient, $\mathsf{X}_k(\mathsf{H}, \mathsf{n}_0)$, generally depending on H and the perturbation matrix n_0 up to some (possibly infinite) r. The singularity is characterized by the order $s \in \mathbb{N}_+$ of the pole in the SM expansion, which for any G_{θ_0} is found by a recursive procedure [57]. Equation (14) implies then $\boldsymbol{\mathcal{F}}_{00} \approx \theta_0^{-2s}[A + \mathcal{O}(\theta_0)]$ for some θ_0-independent $A > 0$ [57], so the error $\delta_{\mathrm{Q}}\theta_0 = 1/\sqrt{\boldsymbol{\mathcal{F}}_{00}} \propto \theta_0^s$ vanishes as $\theta_0 \to 0$ at a rate dictated by s. This proves the singularity of H to be essential for unbounded sensitivity, while other system properties, e.g. exhibiting an EP and/or balancing the loss and gain rates [31], can only play a role in determining the pole-order s. For the system considered, we evaluate the SM expansions for the choices of the perturbation matrix n_0 listed below Eq. (5) [57]. We observe that only in the case of two-mode symmetric frequency perturbations, $\mathsf{n}_0 = \mathsf{I}$ [31], the pole is second order, while in all other cases it is of order one. We focus on the former in Fig. 3, where we plot the exact, numerically obtained, estimation error (black lines)—neither noisy (14) nor $\theta_0 \approx 0$ approximations are made—that consistently follows a quadratic scaling.

Impact of nuisance parameters.—Dealing with the multiparameter scenario, in order to expand the response function (8) around $\theta_0 = 0$, it is now $\mathsf{H}_{\bar{\boldsymbol{\theta}}}$ appearing in Eq. (8) whose singularity must be verified. Still, when $\mathsf{H}_{\bar{\boldsymbol{\theta}}}$ is nonsingular, $\mathsf{G}_{\boldsymbol{\theta}}$ admits again a Neumann series with $\lim_{\theta_0\to 0}\mathsf{G}_{\boldsymbol{\theta}} = -\mathsf{J}\mathsf{H}^{-1}_{\bar{\boldsymbol{\theta}}}$. Hence, $\boldsymbol{\mathcal{F}}_{00}$ must be bounded as before, with the estimation error $\Delta_{\mathrm{Q}}\theta_0 = \sqrt{[\boldsymbol{\mathcal{F}}^{-1}]_{00}} \geq 1/\boldsymbol{\mathcal{F}}_{00}$ forbidden to vanish as $\theta_0 \to 0$. When $\mathsf{H}_{\bar{\boldsymbol{\theta}}}$ is singular instead, it is the SM expansion of $\mathsf{G}_{\boldsymbol{\theta}}$ that is valid, with the expansion coefficients X_k depending now also on nuisance parameters $\bar{\boldsymbol{\theta}}$. However, the sensitivity scaling in θ_0 may not be associated with the pole order any more, as the error $\Delta_{\mathrm{Q}}\theta_0 = \sqrt{[\boldsymbol{\mathcal{F}}^{-1}]_{00}}$ involves the inverse of the QFIM and, hence, is generally affected by correlations between different unknown parameters. We show this explicitly by focusing on the two-parameter estimation scenario with

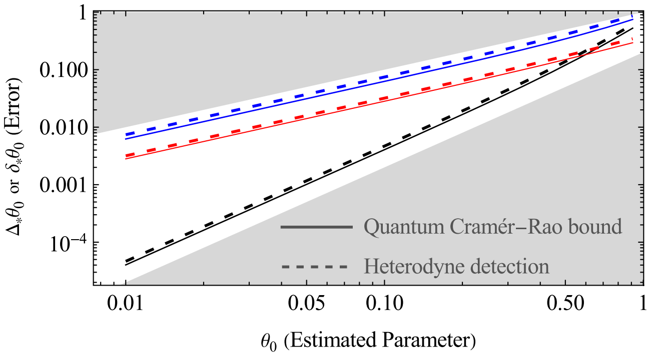

FIG. 3. Estimation errors attained by heterodyne detection (dashed lines), $\delta_C\theta_0$ or $\Delta_C\theta_0$, vs quantum Cramér-Rao bounds applicable to any measurement (solid lines), $\delta_Q\theta_0$ or $\Delta_Q\theta_0$. Within the ideal single-parameter scenario, both $\delta_*\theta_0$ (black) follow quadratic scaling. When θ_1 constitutes a nuisance parameter whose variations maintain the singularity, the estimation errors $\Delta_*\theta_0$ scale linearly with θ_0, e.g. for $\theta_1 = 0$ (red) or $\theta_1 = 0.25$ (blue). In the above, all probe and scattering input modes are chosen to be in a thermal state with average photon-number $n_A = n_B = 1$, while the intermode couplings are set to $\kappa = g = 1$ and $\eta_1 = 1$, $\eta_2 = 3$.

the primary θ_0 generated by $\mathsf{n}_0 = \mathsf{I}$, while θ_1 acts as nuisance parameter of either $\mathbf{H}^{\mathrm{NS}}_{\theta_1}$ or $\mathbf{H}^{\mathrm{S}}_{\theta_1}$ in Eq. (9)—black or red arrows in Fig. 2(a).

In case of $\mathbf{H}^{\mathrm{NS}}_{\theta_1}$, the error in estimating θ_0 may not vanish as $\theta_0 \to 0$ for any $\theta_1 \neq 0$, for which H_{θ_1} is *nonsingular*. We show this explicitly by considering a thermal state with zero displacement as the probe input, for which $[\boldsymbol{\mathcal{F}}^{-1}]_{00} = 1/\boldsymbol{\mathcal{F}}_{00} \propto \theta_1^2$ at $\theta_0 = 0$ [57]. At the singular point $\theta_1 = 0$, we also show—by resorting to the SM expansion—that $\Delta_Q\theta_0 = \delta_Q\theta_0 + O(\theta_0^4)$ [57], with the impact of the nuisance parameter being then ignorable and single-parameter results being applicable ($\delta_Q\theta_0 \propto \theta_0^2$, black lines in Fig. 3). Turning to $\mathbf{H}^{\mathrm{S}}_{\theta_1}$, which importantly leads to H_{θ_1} being *singular* for any θ_1, we show that the SM expansion $\mathsf{G}_{\theta_0,\theta_1} = \mathsf{J}\theta_0^{-2}\sum_{k=0}^{1}\theta_0^k \mathsf{X}_k(\theta_1)$ exhibits a second-order pole [57]. Substituting the expansion into Eq. (14), we obtain the entries of QFIM: $\boldsymbol{\mathcal{F}}_{00} \approx \alpha\theta_0^{-4} + 2\beta\theta_0^{-3} + \gamma\theta_0^{-2}$, $\boldsymbol{\mathcal{F}}_{11} \approx \alpha\theta_0^{-2}$, and $\boldsymbol{\mathcal{F}}_{01} \approx \alpha\theta_0^{-3} + \beta\theta_0^{-2}$, with $\alpha, \gamma > 0$ and $\beta \in \mathbb{R}$ [57]. This implies that the error in estimating the primary parameter reads

$$\Delta_Q\theta_0 = \left(\boldsymbol{\mathcal{F}}_{00} - \frac{\boldsymbol{\mathcal{F}}_{01}\boldsymbol{\mathcal{F}}_{10}}{\boldsymbol{\mathcal{F}}_{11}}\right)^{-\frac{1}{2}} \approx \left(\gamma - \frac{\beta^2}{\alpha}\right)^{-\frac{1}{2}}\theta_0, \qquad (15)$$

and scales linearly with θ_0—the presence of nuisance θ_1 precludes the scaling from following the quadratic behavior dictated by the pole. We show this explicitly in Fig. 3, where we plot the exact estimation error $\Delta_Q\theta_0$ in red (blue) for $\mathbf{H}^{\mathrm{S}}_{\theta_1}$ with $\theta_1 = 0$ ($\theta_1 = 0.25$), as well as $\Delta_C\theta_0$ attained by heterodyne detection (dashed lines) that also follow the linear scaling.

Conclusions.—We establish the tools necessary to assess quantum Gaussian systems in sensing linear perturbations away from singularities. We investigate the divergence of sensitivity then exhibited, while clarifying that other dynamical properties, e.g. operation at an exceptional point, fulfilment of lasing conditions or nonreciprocity, do not play a primary role. However, we demonstrate that nuisance parameters may then strongly affect the performance, i.e. the rate at which the sensitivity diverges. Such a phenomenon resembles the setting of quantum superresolution problems [80], in which the lack of a spatial reference disallows one resolving infinitesimal separations between objects [81–85]. We leave open the question of how our results change, if one accounts for any prior knowledge about the sensed and/or nuisance parameters [86–88].

We thank Dayou Yang, Mădălin Guţă, Marcin Jarzyna, Mohammad Mehboudi, Giacomo Sorelli, and Konrad Banaszek for helpful comments. This work has been supported by the Quantum Optical Technologies project that is carried out within the International Research Agendas program of the Foundation for Polish Science cofinanced by the European Union under the European Regional Development Fund. R. W. C. also acknowledges support from the Polish National Science Centre (NCN) under the Maestro Grant No. DEC-2019/34/A/ST2/00081.

*j.naikoo@cent.uw.edu.pl
†jan.kolodynski@cent.uw.edu.pl

[1] C. L. Degen, F. Reinhard, and P. Cappellaro, Rev. Mod. Phys. **89**, 035002 (2017).
[2] L. Pezzè, A. Smerzi, M. K. Oberthaler, R. Schmied, and P. Treutlein, Rev. Mod. Phys. **90**, 035005 (2018).
[3] V. Giovannetti, S. Lloyd, and L. Maccone, Science **306**, 1330 (2004).
[4] L. Maccone and V. Giovannetti, Nat. Phys. **7**, 376 (2011).
[5] B. M. Escher, R. L. de Matos Filho, and L. Davidovich, Nat. Phys. **7**, 406 (2011).
[6] R. Demkowicz-Dobrzański, J. Kołodyński, and M. Guţă, Nat. Commun. **3**, 1063 (2012).
[7] R. Chaves, J. B. Brask, M. Markiewicz, J. Kołodyński, and A. Acin, Phys. Rev. Lett. **111**, 120401 (2013).
[8] Y. L. Len, T. Gefen, A. Retzker, and J. Kołodyński, Nat. Commun. **13**, 6971 (2022).
[9] K. Yamamoto, S. Endo, H. Hakoshima, Y. Matsuzaki, and Y. Tokunaga, Phys. Rev. Lett. **129**, 250503 (2022).
[10] P. Sekatski, M. Skotiniotis, J. Kołodyński, and W. Dür, Quantum **1**, 27 (2017).
[11] S. Zhou, M. Zhang, J. Preskill, and L. Jiang, Nat. Commun. **9**, 78 (2018).
[12] R. Demkowicz-Dobrzański, J. Czajkowski, and P. Sekatski, Phys. Rev. X **7**, 041009 (2017).
[13] J. Wiersig, Phys. Rev. Lett. **112**, 203901 (2014).
[14] W. D. Heiss, J. Phys. A **37**, 2455 (2004).

[15] M. A. Miri and A. Alù, Science **363**, eaar7709 (2019).
[16] F. Minganti, A. Miranowicz, R. W. Chhajlany, and F. Nori, Phys. Rev. A **100**, 062131 (2019).
[17] J. Wiersig, Photonics Res. **8**, 1457 (2020).
[18] W. Chen, Ş. Kaya Özdemir, G. Zhao, J. Wiersig, and L. Yang, Nature (London) **548**, 192 (2017).
[19] H. Hodaei, A. U. Hassan, S. Wittek, H. Garcia-Gracia, R. El-Ganainy, D. N. Christodoulides, and M. Khajavikhan, Nature (London) **548**, 187 (2017).
[20] C. Chen, L. Jin, and R.-B. Liu, New J. Phys. **21**, 083002 (2019).
[21] J. Wiersig, Nat. Commun. **11**, 2454 (2020).
[22] H. Wang, Y. H. Lai, Z. Yuan, M. G. Suh, and K. Vahala, Nat. Commun. **11**, 1 (2020).
[23] A. A. Clerk, M. H. Devoret, S. M. Girvin, F. Marquardt, and R. J. Schoelkopf, Rev. Mod. Phys. **82**, 1155 (2010).
[24] M. Tsang, Opt. Lett. **43**, 150 (2018).
[25] R. Kononchuk, J. Cai, F. Ellis, R. Thevamaran, and T. Kottos, Nature (London) **607**, 697 (2022).
[26] C. W. Gardiner and M. J. Collett, Phys. Rev. A **31**, 3761 (1985).
[27] See Ref. [28] for considerations of also finite dimensional systems.
[28] Y. Chu, Y. Liu, H. Liu, and J. Cai, Phys. Rev. Lett. **124**, 020501 (2020).
[29] H.-K. Lau and A. A. Clerk, Nat. Commun. **9**, 1 (2018).
[30] Reference [31] attributed this to EP and lasing-threshold conditions, while actually satisfying the singularity condition [20].
[31] M. Zhang, W. Sweeney, C. W. Hsu, L. Yang, A. D. Stone, and L. Jiang, Phys. Rev. Lett. **123**, 180501 (2019).
[32] K. Macieszczak, M. Guţă, I. Lesanovsky, and J. P. Garrahan, Phys. Rev. A **93**, 022103 (2016).
[33] S. Fernández-Lorenzo and D. Porras, Phys. Rev. A **96**, 013817 (2017).
[34] S. Wald, S. V. Moreira, and F. L. Semião, Phys. Rev. E **101**, 052107 (2020).
[35] Y. Chu, S. Zhang, B. Yu, and J. Cai, Phys. Rev. Lett. **126**, 010502 (2021).
[36] W. Wu and C. Shi, Phys. Rev. A **104**, 022612 (2021).
[37] D. Xie, C. Xu, and A. M. Wang, Eur. Phys. J. Plus **137**, 1323 (2022).
[38] R. Di Candia, F. Minganti, K. V. Petrovnin, G. S. Paraoanu, and S. Felicetti, npj Quantum Inf. **9**, 23 (2023).
[39] T. Ilias, D. Yang, S. F. Huelga, and M. B. Plenio, PRX Quantum **3**, 010354 (2022).
[40] B. Peng, Ş. K. Özdemir, F. Lei, F. Monifi, M. Gianfreda, G. L. Long, S. Fan, F. Nori, C. M. Bender, and L. Yang, Nat. Phys. **10**, 394 (2014).
[41] H. Hodaei, M.-A. Miri, M. Heinrich, D. N. Christodoulides, and M. Khajavikhan, Science **346**, 975 (2014).
[42] L. Feng, Z. J. Wong, R.-M. Ma, Y. Wang, and X. Zhang, Science **346**, 972 (2014).
[43] B. Peng, Ş. K. Özdemir, S. Rotter, H. Yilmaz, M. Liertzer, F. Monifi, C. M. Bender, F. Nori, and L. Yang, Science **346**, 328 (2014).
[44] M. Partanen, J. Goetz, K. Y. Tan, K. Kohvakka, V. Sevriuk, R. E. Lake, R. Kokkoniemi, J. Ikonen, D. Hazra, A. Mäkinen, E. Hyyppä, L. Grönberg, V. Vesterinen, M. Silveri, and M. Möttönen, Phys. Rev. B **100**, 134505 (2019).
[45] R. El-Ganainy, K. G. Makris, M. Khajavikhan, Z. H. Musslimani, S. Rotter, and D. N. Christodoulides, Nat. Phys. **14**, 11 (2018).
[46] R. Nichols, P. Liuzzo-Scorpo, P. A. Knott, and G. Adesso, Phys. Rev. A **98**, 012114 (2018).
[47] M. Sain and J. Massey, IEEE Trans. Autom. Control **14**, 141 (1969).
[48] P. G. Howlett, J. Aust. Math. Soc. Series B, Appl. Math. **23**, 357 (1982).
[49] P. Howlett and K. Avrachenkov, in *Optimization and Related Topics*, edited by A. Rubinov and B. Glover (Springer, Boston, MA, 2001), pp. 325–342.
[50] K. E. Avrachenkov, J. A. Filar, and P. G. Howlett, *Analytic Perturbation Theory and Its Applications* (SIAM, Philadelphia, 2013).
[51] R. Demkowicz-Dobrzański, W. Górecki, and M. Guţă, J. Phys. A **53**, 363001 (2020).
[52] J. Suzuki, Y. Yang, and M. Hayashi, J. Phys. A **53**, 453001 (2020).
[53] A. A. Clerk, M. H. Devoret, S. M. Girvin, F. Marquardt, and R. J. Schoelkopf, Rev. Mod. Phys. **82**, 1155 (2010).
[54] A. W. Bruch, X. Liu, J. B. Surya, C.-L. Zou, and H. X. Tang, Optica **6**, 1361 (2019).
[55] C. Gardiner and P. Zoller, *Quantum Noise: A Handbook of Markovian and Non-Markovian Quantum Stochastic Methods with Applications to Quantum Optics*, Springer Series in Synergetics (Springer, Berlin Heidelberg, 2010).
[56] M. Guţă and N. Yamamoto, IEEE Trans. Autom. Control **61**, 921 (2016).
[57] See Supplemental Material at http://link.aps.org/supplemental/10.1103/PhysRevLett.131.220801 for the derivation of the system Gaussian dynamics, as well as its consequences in sensing tasks when operating the system at a singularity or other special dynamical points, e.g., the lasing threshold.
[58] We do not exclude possibility of non-Gaussian measurements.
[59] A. Ferraro, S. Olivares, and M. G. A. Paris, *Gaussian States in Continuous Variable Quantum Information* (Bibliopolis, Napoli, 2005), arXiv:quant-ph/0503237.
[60] C. Weedbrook, S. Pirandola, R. Garcia-Patrón, N. J. Cerf, T. C. Ralph, J. H. Shapiro, and S. Lloyd, Rev. Mod. Phys. **84**, 621 (2012).
[61] Phase-space representation of a matrix m reads $\mathsf{m} \equiv \mathcal{J}\{m\} \coloneqq (\mathrm{Re}[m], -\mathrm{Im}[m]; \mathrm{Im}[m], \mathrm{Re}[m])$, e.g. $\mathsf{J} \coloneqq \mathcal{J}\{iI\}$.
[62] For $\omega \neq \omega_0$, the response function (6) can be made divergent only for a balanced system, $\gamma_1 = \gamma_2 = \gamma$, with strong coupling $g = \sqrt{\gamma^2 + (\omega - \omega_0)^2} > \gamma$ [57].
[63] Maintenance of EP is not essential when not restricted to PT-preserving perturbations.
[64] Any value of $\chi > 0$ such that $g = \gamma_1 = \gamma_2 = \chi$ can be rescaled to $\chi = 1$ by redefining the perturbation parameters θ_j.
[65] C. W. Helstrom, *Quantum Detection and Estimation Theory* (Academic Press, New York, 1976).
[66] A. S. Holevo, *Probabilistic and Statistical Aspects of Quantum Theory* (North Holland, Amsterdam, 1982).
[67] S. L. Braunstein and C. M. Caves, Phys. Rev. Lett. **72**, 3439 (1994).
[68] S. Ragy, M. Jarzyna, and R. Demkowicz-Dobrzański, Phys. Rev. A **94**, 052108 (2016).

[69] For $\boldsymbol{W}_{jk} = \delta_{ij}\delta_{ik}$ an θ_i estimator and optimal measurement are guaranteed to exist such that $\nu\Delta^2\tilde{\theta}_i = \Delta^2_{\mathrm{C}}\theta_i = \Delta^2_{\mathrm{Q}}\theta_i$ [70].
[70] W. Górecki, arXiv:2304.14370.
[71] M. F. B. Cenni, L. Lami, A. Acin, and M. Mehboudi, Quantum **6**, 743 (2022).
[72] S. M. Kay, *Fundamentals of Statistical Signal Processing: Estimation Theory* (Prentice-Hall, Inc., New York, 1993).
[73] A. Monras and F. Illuminati, Phys. Rev. A **81**, 062326 (2010).
[74] A. Monras, arXiv:1303.3682.
[75] J. Liu, H. Yuan, X.-M. Lu, and X. Wang, J. Phys. A **53**, 023001 (2019).
[76] D. Šafránek, J. Phys. A **52**, 035304 (2018).
[77] Z. Jiang, Phys. Rev. A **89**, 032128 (2014).
[78] Not to be confused with a Taylor expansion in θ_0^{-1} [31], which cannot be trusted [57].
[79] The minimal error may still diminish, e.g., with the mean number of photons, $\bar{n}$, in the probes, for which S_{in}, $\mathsf{V}_{\mathrm{in}} \propto \bar{n}$ and, hence, Eq. (14) yields the standard quantum limit [29], i.e. $\mathcal{F}_{00} \propto \bar{n}$ for $\bar{n} \gg 1$.
[80] M. Tsang, R. Nair, and X.-M. Lu, Phys. Rev. X **6**, 031033 (2016).
[81] A. Chrostowski, R. Demkowicz-Dobrzański, M. Jarzyna, and K. Banaszek, Int. J. Quantum. Inform. **15**, 1740005 (2017).
[82] J. Řehaček, Z. Hradil, B. Stoklasa, M. Paúr, J. Grover, A. Krzic, and L. L. Sánchez-Soto, Phys. Rev. A **96**, 062107 (2017).
[83] M. R. Grace, Z. Dutton, A. Ashok, and S. Guha, J. Opt. Soc. Am. A **37**, 1288 (2020).
[84] G. Sorelli, M. Gessner, M. Walschaers, and N. Treps, Phys. Rev. Lett. **127**, 123604 (2021).
[85] J. O. de Almeida, J. Kołodyński, C. Hirche, M. Lewenstein, and M. Skotiniotis, Phys. Rev. A **103**, 022406 (2021).
[86] J. Rubio and J. Dunningham, Phys. Rev. A **101**, 032114 (2020).
[87] J. Rubio, J. Anders, and L. A. Correa, Phys. Rev. Lett. **127**, 190402 (2021).
[88] M. Mehboudi, M. R. Jørgensen, S. Seah, J. B. Brask, J. Kołodyński, and M. Perarnau-Llobet, Phys. Rev. Lett. **128**, 130502 (2022).